Nonlinear observer design for a Greitzer compressor model

Christoph Josef Backi[1], **Jan Tommy Gravdahl**[2] **and Esten Ingar Grøtli**[3]

Department of Engineering Cybernetics
Norwegian University of Science and Technology
O.S. Bragstads plass 2D, 7034 Trondheim, Norway

Abstract— In this paper two different observers for a non-linear compressor model have been developed and compared: A nonlinear observer based on a circle criterion design and an Extended Kalman Filter. Both of these observers were implemented together with linear control strategies in order to (surge-)control the nonlinear Greitzer compressor model. The newly developed nonlinear observer is a full state observer providing local asymptotic stability results. Compared to the Extended Kalman Filter, the nonlinear observer showed itself at least equivalent, even superior for open-loop estimation.

I. INTRODUCTION

The system that is the basis for this paper is a model of an axial compressor introduced by [5]. If a compressor is operated below a certain mass flow limit called the surge line, it goes into an unstable mode of operation characterized by a limit-cycle oscillation in flow and pressure. This is called surge, which can damage the compressor physically and will in any case lower the performance.

Controlling this phenomenon is vital and one way of doing so is by using a so called close-coupled valve (CCV) introduced by [9]. The CCV directly influences the compressor's characteristics and thus stabilizes the dynamics. The compressor and the CCV can be considered as an extended compressor, meaning that the overall dynamics are comparable to those of a compressor (see Figure 1).

Surge can be controlled for example by state feedback control as well as output feedback control. For an output feedback design for a Moore-Greitzer compressor model, see e.g. [7]. In [8] a robust output feedback controller is presented for active surge control of compression systems. A broad review of surge and rotating stall controllers can be found in [3].

[4] mentions that the most promising way of surge control is by using feedback from mass flow. Due to the fact that mass flow is both difficult and expensive to measure, mass flow observers have been studied before, e.g. in [2], [7] and [8] for more general compression systems. This paper though imposes new results for the Greitzer compressor model, because it provides a full state observer with local stability results, whereas other papers handle only estimation of the nonmeasurable state, e.g. [2].

[1]corresponding author, christoph.backi@itk.ntnu.no
[2]jan.tommy.gravdahl@itk.ntnu.no
[3]esten.grotli@itk.ntnu.no
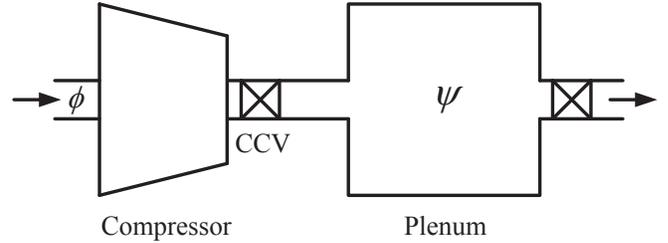
Fig. 1: Compressor with CCV

II. MODEL

The following equations describe the Greitzer axial compressor model and have already been transformed for the origin to be equilibrium point (for details see [4])

$$\dot{\hat{\psi}} = \frac{1}{B} \left(\hat{\phi} - \hat{\Phi}(\hat{\psi}) \right)$$
$$\dot{\hat{\phi}} = B \left(\hat{\Psi}_c(\hat{\phi}) - \hat{\psi} - u \right), \tag{1}$$

where u is the pressure drop across the CCV,

$$\hat{\Psi}_c(\hat{\phi}) = -k_3 \hat{\phi}^3 - k_2 \hat{\phi}^2 - k_1 \hat{\phi} \tag{2}$$

denotes the compressor characteristics and

$$\hat{\Phi}(\hat{\psi}) = \gamma \left(\mathrm{sgn}(\hat{\psi} + \hat{\psi}_0) \sqrt{|\hat{\psi} + \hat{\psi}_0|} - \mathrm{sgn}(\hat{\psi}_0) \sqrt{|\hat{\psi}_0|} \right) \tag{3}$$

denotes the throttle characteristics, where $\hat{\psi}_0$ is always positive. Thus, (3) can be rewritten as

$$\hat{\Phi}(\hat{\psi}) = \gamma \left(\mathrm{sgn}(\hat{\psi} + \hat{\psi}_0) \sqrt{|\hat{\psi} + \hat{\psi}_0|} - \sqrt{\hat{\psi}_0} \right). \tag{4}$$

Note that $\hat{\cdot}$ does not indicate an estimated value, but the displacement from equilibrium points $\hat{\psi} = \psi - \psi_0$ and $\hat{\phi} = \phi - \phi_0$. Further, ϕ describes the mass flow coefficient (axial velocity divided by wheel speed) and ψ describes the non-dimensional pressure coefficient (pressure divided by density and the square of wheel speed). In addition γ denotes the throttle gain and $\mathrm{sgn}(0) = 0$.

For the parameters the following relations hold:
$B = \frac{U}{2a_s} \sqrt{\frac{V_p}{A_c L_c}} > 0$, where U is the compressor speed, a_s is the speed of sound, V_p is the plenum volume, A_c is the flow area, L_c is the length of ducts and compressor, $k_1 = \frac{3H\phi_0}{2W^2} \left(\frac{\phi_0}{W} - 2 \right)$, $k_2 = \frac{3H}{2W^2} \left(\frac{\phi_0}{W} - 1 \right)$ and $k_3 = \frac{H}{2W^3}$, where $H > 0$, $W > 0$ and $\phi_0 > 0$.

Note that in Figure 2 the displayed throttle and compressor characteristics have not been moved to the origin, but it shows how an operating setpoint can be found using the original system model (see [4] for details).
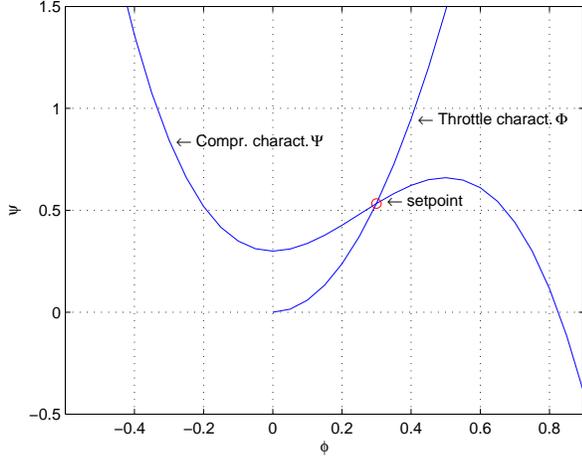
Fig. 2: Throttle and compressor characteristics with setpoint in the surge area

By setting $\hat{\psi} = x_1$, $\hat{\phi} = x_2$, $\psi_0 = x_{1_0}$ and $\phi_0 = x_{2_0}$ the system can be rewritten as

$$\begin{aligned} \dot{x}_1 &= \frac{1}{B}\left(x_2 - \gamma\left(\operatorname{sgn}\left(x_1 + x_{1_0}\right)\sqrt{\left|x_1 + x_{1_0}\right|} - \sqrt{x_{1_0}}\right)\right) \\ \dot{x}_2 &= B\left(-k_3 x_2^3 - k_2 x_2^2 - k_1 x_2 - x_1 - u\right). \end{aligned} \quad (5)$$

The system can be represented in the form $\dot{x} = f(x) + gu$, with $x \in \mathbb{R}^n$, $u \in \mathbb{R}^m$, $n = 2$, $m = 1$ and $g = \begin{bmatrix} 0 & -B \end{bmatrix}^T$. The system's measurable state is x_1 and thus $y = h(x) = Cx$ with $C = \begin{bmatrix} 1 & 0 \end{bmatrix}$.

III. OBSERVABILITY

An observability test of the model (5) based on [6, Definition 5.2.1] leads to a vector of Lie-derivatives

$$J = \begin{bmatrix} L_f^0 h(x) \\ L_f^1 h(x) \end{bmatrix} = \begin{bmatrix} h(x) \\ \frac{\partial h(x)}{\partial x} f(x) \end{bmatrix} = \begin{bmatrix} x_1 \\ \dot{x}_1 \end{bmatrix}$$

for which a gradient operator $\mathscr{O} = \frac{\partial J}{\partial x}$ can be defined. The resulting matrix needs to have full rank for the model (5) to be observable:

$$\mathscr{O} = \begin{bmatrix} 1 & 0 \\ \frac{\gamma}{B}\left(-\delta\left(x_1 + x_{1_0}\right)\sqrt{\left|x_1 + x_{1_0}\right|} - \frac{\operatorname{sgn}(x_1 + x_{1_0})}{2\sqrt{|x_1 + x_{1_0}|}}\right) & \frac{1}{B} \end{bmatrix} \quad (6)$$

with $\delta(\cdot)$ denoting the Dirac delta function. $\mathscr{O}$ has full rank $\forall x_1, x_2 \in \mathbb{R}$ and thus (5) is observable.

IV. CONTROLLER DESIGN

The controller that is chosen to (surge-)control the compressor is a linear controller. In order to prove stability of

the linear controller the assumption is made that all states x_i are available from measurements.

Later in the paper we will prove stability also for feedback of the state estimates $\hat{x}_i$.

A. Proof of Stability

Recalling the compressor's nonlinear equations (5) with the linear control law $u = \mu_1 x_1 + \mu_2 x_2$ results in the closed loop description

$$\begin{aligned} \dot{x}_1 &= \frac{1}{B}\left(x_2 - \gamma\left(\operatorname{sgn}\left(x_1 + x_{1_0}\right)\sqrt{\left|x_1 + x_{1_0}\right|} - \sqrt{x_{1_0}}\right)\right) \\ \dot{x}_2 &= B\left(-k_3 x_2^3 - k_2 x_2^2 - (k_1 + \mu_2) x_2 - (1 + \mu_1) x_1\right). \end{aligned} \quad (7)$$

A Lyapunov function candidate is chosen as $V_C = \frac{1}{2}\left(Bx_1^2 + \frac{1}{B}x_2^2\right)$ which is clearly positive definite $\forall x_1, x_2 \in \mathbb{R}\backslash\{0\}$. Its time derivative $\dot{V}_C = Bx_1\dot{x}_1 + \frac{1}{B}x_2\dot{x}_2$ has to be negative $\forall x_1, x_2 \in \mathbb{R}\backslash\{0\}$:

$$\dot{V}_C = \underbrace{-\mu_1 x_1 x_2}_{\text{I}} - \underbrace{x_1 \gamma\left(\operatorname{sgn}\left(x_1 + x_{1_0}\right)\sqrt{\left|x_1 + x_{1_0}\right|} - \sqrt{x_{1_0}}\right)}_{\text{II}} \\ - x_2^2 \underbrace{\left(k_3 x_2^2 + k_2 x_2 + (k_1 + \mu_2)\right)}_{\text{III}}. \quad (8)$$

$\dot{V}_C < 0$ if the terms I, II and III are each > 0 $\forall x_1, x_2 \in \mathbb{R}\backslash\{0\}$. Term II > 0 $\forall x_1 \in \mathbb{R}$ and $\forall x_{1_0} \in \mathbb{R}^+$.
Term III is a quadratic function depending on the variable x_2, which, to be > 0, may have no zeros (no intersection with the variable's axis). Therefore, the solution of III $= 0$ is calculated as $x_{2_{1,2}} = -\frac{k_2}{2k_3} \pm \sqrt{\frac{k_2^2}{4k_3^2} - \frac{k_1 + \mu_2}{k_3}}$. Thus, for the parabola defined in term III to have no zeros, the square root term $\sqrt{\frac{k_2^2}{4k_3^2} - \frac{k_1 + \mu_2}{k_3}}$ must be a complex number. Thus, the radicand $\frac{k_2^2}{4k_3^2} - \frac{k_1 + \mu_2}{k_3} \overset{!}{<} 0$ which leads to

$$\mu_2 > \frac{k_2^2}{4k_3} - k_1. \quad (9)$$

This only holds, if $k_3 > 0$ (parabola opened upwards), which is the case for the model of the system.

For the Lyapunov function derivative (8) to be negative definite, now the controller gain μ_1 can be set to zero, meaning that term I vanishes. But it is desirable to have feedback from the measurable state x_1 as well and thus an upper bound for (8) can be introduced

$$\dot{V}_C \leq -\mu_1 x_1 x_2 - \beta_1 x_1^2 - \beta_2 x_2^2, \quad (10)$$

where $\beta_i \in \mathbb{R}^+$. From (8) and (10) we find the two expressions $\beta_1 x_1^2 \leq \text{II}$ and $\beta_2 \leq \text{III}$, which hold at least for a small environment around the origin. In this case (10) can be rewritten as

$$\dot{V}_C \leq -x^T Q x = -x^T \begin{bmatrix} \beta_1 & \frac{\mu_1}{2} \\ \frac{\mu_1}{2} & \beta_2 \end{bmatrix} x. \quad (11)$$

Q can be made positive (semi-)definite by looking at the

eigenvalues $q_{1,2}$ of Q, which have to be positive. Out of

$$q_{1,2} = \frac{1}{2}\left(\beta_1 + \beta_2 \pm \sqrt{(\beta_1 - \beta_2)^2 + \mu_1^2}\right)$$

the following inequality is received

$$\beta_1 + \beta_2 \geq \sqrt{(\beta_1 - \beta_2)^2 + \mu_1^2}$$

yielding into $\mu_1 \leq \pm 2\sqrt{\beta_1 \beta_2}$ for Q to be positive (semi-) definite. Following a conservative approach the bound on μ_1 is chosen to be $0 < \mu_1 \leq 2\sqrt{\beta_1 \beta_2}$.

A further investigation of the size of the controller gain μ_2 leads to a direct dependence on β_2. We show this by introducing an additional value η in the inequality (9) leading to $\mu_2 = \frac{k_2^2}{4k_3} - k_1 + \eta$ and putting this into the inequality $\beta_2 \leq$ III. By solving this inequality (again we only allow zero or a complex number as solutions), we receive the inequality $\beta_2 \overset{!}{<} \eta$. This is a powerful result due to the fact that now we can design the matrix Q almost only by choosing μ_2: The choice of μ_2 defines a bound on β_2, which itself defines a bound on μ_1.

Finding a value for β_1 analytically out of the inequality $\beta_1 x_1^2 \leq$ II is harder and has been done by trial-and-error–simulation for the parameter ranges $-5 \leq x_1 \leq 5$ and $0 \leq x_{1_0} \leq 0.5$. A value of $\beta_1 = 0.3$ has been found to be suiting the problem (see the error plot II $- \beta_1 x_1^2 \geq 0$ in Figure 3). Due to the fact that β_1 is fixed now, a design of the matrix Q is just depending on the choice of μ_2.
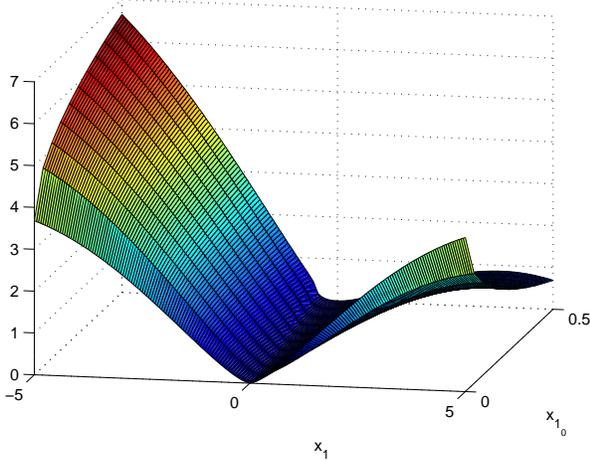
Fig. 3: Error plot of II $- \beta_1 x_1^2$ for $\beta_1 = 0.3$

If all these requirements on the elements of the matrix Q are fulfilled, we have obtained a locally asymptotically stable state feedback controller. It has to be mentioned that, the smaller β_1 gets chosen, the bigger the range of x_1 can be set and thus the local asymptotical stability result becomes more powerful. Nevertheless, the range $-5 \leq x_1 \leq 5$ is sufficient for the application presented in this paper.

V. NONLINEAR OBSERVER

In this section we propose a nonlinear observer based on the circle criterion design as introduced in [1].

A. Theory

For the design the system's equations (5) can be written into the following form:

$$\begin{aligned}\dot{x} &= A_{CC}x + G\xi\left(\Upsilon x\right) + \rho\left(y, u\right)\\ y &= Cx\end{aligned} \tag{12}$$

With

$$A_{CC} = \begin{bmatrix} 0 & 1/B \\ -B & -\varepsilon B \end{bmatrix}, \tag{13}$$

$$C = \begin{bmatrix} 1 & 0 \end{bmatrix}, \Upsilon = \begin{bmatrix} 0 & 1 \end{bmatrix}, G = \begin{bmatrix} 0 \\ -B \end{bmatrix}, \tag{14}$$

$$\rho\left(y, u\right) = \begin{bmatrix} -\gamma\left(\text{sgn}\left(x_1 + x_{1_0}\right)\sqrt{|x_1 + x_{1_0}|} - \sqrt{x_{1_0}}\right) \\ -Bu, \end{bmatrix} \tag{15}$$

$$\xi\left(x_2\right) = k_3 x_2^3 + k_2 x_2^2 - \left(\varepsilon - k_1\right)x_2 \tag{16}$$

where ε is chosen such that the polynomial (16) is nondecreasing for all feasible values of k_1.

It has to hold that the pair (A_{CC}, C) is detectable. Further $\xi\left(\cdot\right)$ and $\rho\left(\cdot, \cdot\right)$ are locally Lipschitz. The main restriction is that $\xi\left(\cdot\right)$ is nondecreasing, which means that $(a - b)\left[\xi\left(a\right) - \xi\left(b\right)\right] \geq 0 \; \forall a, b \in \mathbb{R}$.

We now design the observer as

$$\dot{\hat{x}} = A_{CC}\hat{x} + L\left(C\hat{x} - y\right) + G\xi\left(\Upsilon\hat{x} + K\left(C\hat{x} - y\right)\right) + \rho\left(y, u\right). \tag{17}$$

Thus, the observer error dynamics $\dot{\tilde{x}} = \dot{x} - \dot{\hat{x}}$ are governed by

$$\dot{\tilde{x}} = \left(A_{CC} + LC\right)\tilde{x} + G\left[\underbrace{\xi\left(\Upsilon x\right) - \xi\left(\Upsilon\hat{x} + K\left(C\hat{x} - y\right)\right)}_{\varphi}\right]. \tag{18}$$

Now the observer can be designed by representing the observer error as a linear system with a sector nonlinearity as feedback. The function φ of (18) can now be represented as as a function of Υx and $z := \Upsilon x - \left(\Upsilon\hat{x} + K\left(C\hat{x} - y\right)\right) = \left(\Upsilon + KC\right)\tilde{x}$, which is in fact a time varying nonlinearity in z, so $\varphi := \varphi\left(t, z\right)$. Therefore, the error system can be rewritten into the form

$$\begin{aligned}\dot{\tilde{x}} &= \left(A_{CC} + LC\right)\tilde{x} + G\varphi\left(t, z\right),\\ z &= \left(\Upsilon + KC\right)\tilde{x}\end{aligned} \tag{19}$$

where $\varphi\left(t, z\right)$ has to satisfy $z\varphi\left(t, z\right) \geq 0 \; \forall z \in \mathbb{R}$, meaning it is nondecreasing.

The nonlinear observer designed with the circle criterion is asymptotically stable, if the LMI

$$\begin{bmatrix} \left(A_{CC} + LC\right)^T P + P\left(A_{CC} + LC\right) + \nu I & PG + \left(\Upsilon + KC\right)^T \Lambda \\ G^T P + \Lambda\left(\Upsilon + KC\right) & 0 \end{bmatrix} \leq 0 \tag{20}$$

in P, PL, Λ, ΛK and v is solvable for the matrix $P = P^T > 0$, the constant $v > 0$ and the diagonal matrix $\Lambda > 0$.

For a detailed theoretical study please see [1].

B. Prerequisites

Like already mentioned in subsection V-A the pair (A_{CC}, C) must be detectable, which is fulfilled because the observability matrix has full rank $\begin{bmatrix} C \\ CA_{CC} \end{bmatrix} = \begin{bmatrix} 1 & 0 \\ 0 & 1/B \end{bmatrix}$.
Further, (16) has to be nondecreasing, which will be shown by differentiation:

$$\frac{d}{dx_2} \xi(x_2) = 3k_3 x_2^2 + 2k_2 x_2 - (\varepsilon - k_1) \overset{!}{\geq} 0$$

meaning that no real solutions are allowed for this quadratic equation. The solution to the quadratic inequality in x_2 is

$$x_{2_{1,2}} = -\frac{k_2}{3k_3} \pm \sqrt{\frac{k_2^2}{9k_3^2} + \frac{\varepsilon - k_1}{3k_3}}.$$

For this expression to have no real solution it must hold that the radicand $k_2^2 + 3k_3(\varepsilon - k_1) \leq 0$ or rewritten in terms of k_1, k_2 and k_3 being functions of the setpoint x_{2_0} and / or the constants H and W:

$$\left(\frac{3H}{2W^2} \left(\frac{x_{2_0}}{W} - 1 \right) \right)^2 + \frac{3H}{2W^3} \left(\varepsilon - \frac{3Hx_{2_0}}{2W^2} \left(\frac{x_{2_0}}{W} - 2 \right) \right) \leq 0$$

which is independent of the setpoint x_{2_0} leading to the expression

$$\varepsilon \leq -\frac{3H}{2W}. \tag{21}$$

This means that the polynomial (16) has no extreme values for any values of x_2 and x_{2_0}, if (21) holds. This constitutes a sufficient condition for the demanded property of (16) to be nondecreasing and it can be shown by trivial calculus that this property actually holds.

Due to the fact that the the polynomial (16) is nondecreasing for all x_2 and x_{2_0} it is automatically implied that it is also globally Lipschitz for all x_2 and x_{2_0}, respectively. One could argue in addition that (16) is continuously differentiable and thus at least locally Lipschitz, which is the originally demanded property.

Further, it can be shown that the function (15) is Lipschitz on the set $x_1 \in \mathbb{R} \setminus \{-x_{1_0}\}$, which is the demanded local result.

C. Stability

We are going to prove closed loop asymptotic stability for the system model in connection with the nonlinear observer and the controller. Hereby we use a Lyapunov-approach, which will deliver a local result (due to the fact that the controller delivers a local result).

For the closed loop system controlled by the linear controller we are using the same approach used in subsection IV-A. But now the states in the control law get replaced by their estimates, leading to $u = \mu_1 \hat{x}_1 + \mu_2 \hat{x}_2$. This can be rewritten in state and state-error variables resulting in

$u = \mu_1(x_1 - \tilde{x}_1) + \mu_2(x_2 - \tilde{x}_2)$. Thus, we receive the same closed loop description like in (7), but with an additional vectorial term $\tilde{g}(\tilde{x}_1, \tilde{x}_2) = \begin{bmatrix} 0 \\ B(\mu_1 \tilde{x}_1 + \mu_2 \tilde{x}_2) \end{bmatrix}$.
Now we take the same Lyapunov function candidate $V_1 = \frac{1}{2}\left(Bx_1^2 + \frac{1}{B}x_2^2\right)$ which has already been defined in subsection IV-A. Thus the time-derivative of V_1 with feedback of the observer-states becomes

$$\dot{V}_1 = \dot{V}_C + \mu_1 \tilde{x}_1 x_2 + \mu_2 \tilde{x}_2 x_2 \tag{22}$$

where $\dot{V}_C$ is defined in (8).

In [1, Theorem 1] a Lyapunov function candidate for the observer error is defined as $V_2 = \tilde{x}^T P \tilde{x}$ where P is delivered out of the solution of the LMI defined in (20). The authors of [1] show that the time derivative of this Lyapunov function is less or equal than some upper bound $\dot{V}_2 \leq -v\tilde{x}^T \tilde{x}$, where v comes out of the solution of the LMI as well.

Now we can define a Lyapunov function candidate for the overall system as $V = V_1 + V_2$ with its time-derivative

$$\dot{V} \leq -x^T Q x + \mu_1 \tilde{x}_1 x_2 + \mu_2 \tilde{x}_2 x_2 - v\tilde{x}^T \tilde{x} \tag{23}$$

to which we now impose an upper bound with the help of Young's inequality:

$$\dot{V} \leq -x^T Q x + \mu_1 \left(\frac{\tilde{x}_1^2}{2} + \frac{x_2^2}{2} \right) + \mu_2 \left(\frac{\tilde{x}_2^2}{2} + \frac{x_2^2}{2} \right) - v\tilde{x}^T \tilde{x}. \tag{24}$$

This can be rewritten into the form $\dot{V} \leq -\check{x}^T \check{Q} \check{x}$ with

$$\check{x}^T = \begin{bmatrix} x_1 & x_2 & \tilde{x}_1 & \tilde{x}_2 \end{bmatrix}^T,$$

$$\check{Q} = \begin{bmatrix} \beta_1 & \mu_1/2 & 0 & 0 \\ \mu_1/2 & \beta_2 - \mu_1/2 - \mu_2/2 & 0 & 0 \\ 0 & 0 & v - \mu_1/2 & 0 \\ 0 & 0 & 0 & v - \mu_2/2 \end{bmatrix}. \tag{25}$$

Now the matrix $\check{Q}$ has to become positive definite by the right choice of variables. Basically one can use Sylvester's criterion, which says that all principal minors of a matrix must be positive for the matrix to be positive definite. In our case this means that if we can make the determinant of the upper left 2–by–2 corner positive, we simply can set a bound on $v \geq v_{bound}$ in the LMI, so that $v_{bound} \geq \mu_1/2$ and $v_{bound} \geq \mu_2/2$. Thus, the matrix $\check{Q}$ will be positive definite.

VI. EXTENDED KALMAN FILTER

The Extended Kalman Filter is an observer based on the Kalman Filter. The basis for this observer is a linearization of the system model (5).

The regular Kalman Filter is linearized around a fixed setpoint and has therefore a constant observer matrix A_{EKF}. In contrary, the Extended Kalman Filter is linearized around moving and thus changing setpoints, leading to a time-dependent observer matrix $A_{EKF}(t)$.

A. Linearization

The linearization of the system model (5) leads to the following observer matrix

$$A_{EKF} = \begin{bmatrix} -\dfrac{\gamma \, \mathrm{sgn}\left(x_{1_S}+x_{1_0}\right)}{2B\sqrt{\left|x_{1_S}+x_{1_0}\right|}} & 1/B \\ -B & B\left(-3k_3 x_{2_S}^2 - 2k_2 x_{2_S} - k_1\right) \end{bmatrix}$$

(26)

with x_{i_S} representing the actual point in state space the compressor is operating in and x_{i_0} representing the desired operating point, like already mentioned in Section II.

Note that $x_{1_S} = \hat{x}_1 = x_1$ (due to the fact that it is measurable) and $x_{2_S} = \hat{x}_2$. Note further that the term $-\delta\left(x_1+x_{1_0}\right)\sqrt{\left|x_1+x_{1_0}\right|}$ (see (6)) is neglected in (26), due to the fact that the case $x_1 = -x_{1_0}$ does not occur in practice.

B. Definition of the Extended Kalman Filter

The following model for the dynamics of the EKF has been chosen (without denoting time dependencies explicitly)

$$\dot{\hat{x}} = (A_{EKF} - L_{EKF}C)\hat{x} + L_{EKF}Cx + gu + G_{EKF}w,$$
$$y = C\hat{x} + v,$$

(27)

including modeling / process and measurement errors as gaussian white noise, denoted as scalars w and v, respectively. Further, $L_{EKF} = \begin{bmatrix} L_{1_{EKF}} & L_{2_{EKF}} \end{bmatrix}^T$, $C = \begin{bmatrix} 1 & 0 \end{bmatrix}$ and $g = \begin{bmatrix} 0 & -B \end{bmatrix}^T$. The process noise is fed into the model with $G_{EKF} = \begin{bmatrix} 1 & 1 \end{bmatrix}^T$. It holds for the expected values that $E(w) = E(v) = 0$, $E\left(ww^T\right) = Q_{EKF} = \mathrm{diag}\left(q_{EKF_1}, q_{EKF_2}\right)$, $E\left(vv^T\right) = R_{EKF} = r_1$ and $E\left(wv^T\right) = N_{EKF} = \begin{bmatrix} 0 & 0 \end{bmatrix}^T$.

The meaning of the elements of Q_{EKF} is that for large values of q_{EKF_i} either the state x_i is heavily influenced by disturbances and / or the model for this state is particularly uncertain. Large values for the element r_1 in R_{EKF} mean that there is a lot of noise present in the measurement of the output y. N_{EKF} is mostly set to zero, because there is no covariance expected between process noise and measurement noise. Further, large Q_{EKF} in relation to R_{EKF} means that the measurement is considered more trustful than the model; and vice versa.

A time-dependent Riccati-Differential-Equation in $P_{EKF}(t)$ has to be solved in order to calculate the observer gains $L_{EKF}(t)$. The time dependence is due to the time dependence of $A_{EKF}(t)$ and thus to the changing setpoints.

$$\dot{P}_{EKF}(t) = A_{EKF}(t)P_{EKF}(t) + P_{EKF}(t)A_{EKF}^T(t)$$
$$- P_{EKF}(t)C^T\frac{1}{r_1}CP_{EKF}(t) + Q_{EKF},$$
$$P_{EKF}(0) = 0,$$
$$L_{EKF}(t) = P_{EKF}(t)C^T\frac{1}{r_1}.$$

(28)

VII. SIMULATIONS

In this section we are presenting different simulation results for both designed observers with the parameters that can be found in the table in the Appendix.

First of all we are going to show how the closed loop systems react on an error in the state x_1 and x_2 respectively. Then we are going to present simulations of diverging initial conditions for the system model and the observers. Finally a simulation with no active controller and a comparison of the estimation during surge will be presented.

The setpoint x_{1_0}, x_{2_0} for all simulations is inside the surge area (see Figure 2 where it is marked).

A. Error in x_1

Figures 4 and 5 show how the closed loop systems with nonlinear observer and Extended Kalman Filter react on an error in the state $x_1 = 0.1$ at $t = 1$ s. The error gets brought back to zero in finite time.

It is remarkable that the observer gains L_{EKF} of the EKF depend on the actual state of the system model / observer and thus change after the error is introduced. For this case both observers don't differ much in their closed loop performance. For both observers a mismatch not only in magnitude but also in sign is viewable between the states x_2 and $\hat{x}_2$.
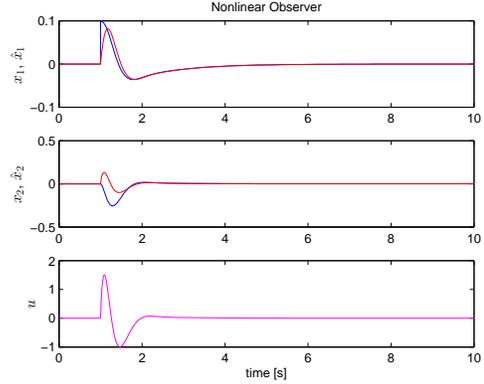
Fig. 4: blue: real states, red: estimated states
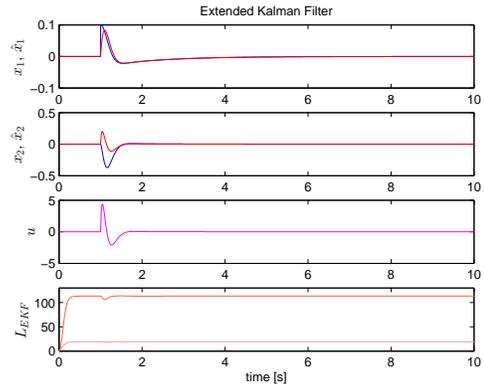
Fig. 5: blue: real states, red: estimated states

B. Error in x_2

In Figures 6 and 7 one can see the closed loop behavior of both observers with controllers for a disturbance in the non-measurable state $x_2 = 0.1$ at $t = 1$ s. Again, the error

gets brought back to zero in finite time for both observers. Although it is not viewable due to the scale of the plot, the observer gains L_{EKF} get adapted due to the change in the actual state of the system model / EKF.

This study is just of theoretical nature and shall visualize the ability of the observers to estimate also the non-measurable state x_2.

Due to the fact that the state x_1 is measurable, it is estimated quite well. But for state x_2 we can see a transiently mismatch between state x_2 and $\hat{x}_2$. This holds for both observers.
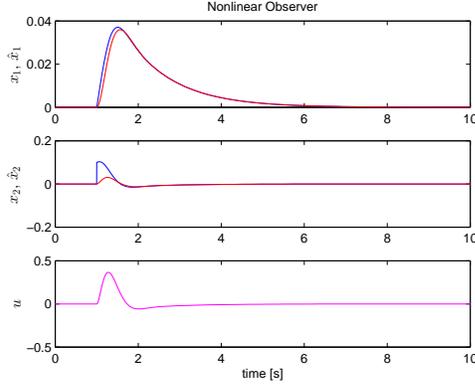
Fig. 6: blue: real states, red: estimated states
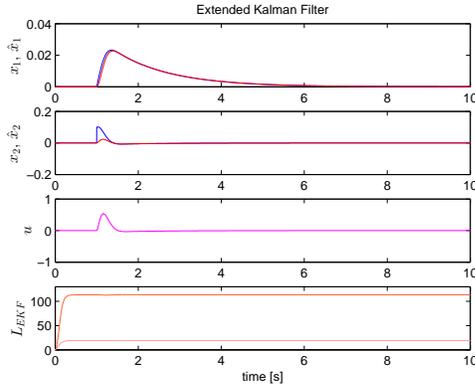
Fig. 7: blue: real states, red: estimated states

C. Diverging initial conditions

Both observers get presented for their performance under diverging initial conditions $x_{init} = \begin{bmatrix} 1 & 1 \end{bmatrix}^T$ and $\hat{x}_{init} = \begin{bmatrix} -1 & -1 \end{bmatrix}^T$ in Figures 8 and 9. Note that for better clarity the EKF in Figure 9 is presented in the range $t \in [0, 5]$ s.

The states / estimated states are brought back to zero in finite time for both observers. Note that the input values for the nonlinear observer and the EKF are very large and can only be regarded as theoretical results without practical relevance. The employment of saturation could make the input signal feasible, but would in any case affect the stability properties leading to another stability proof.
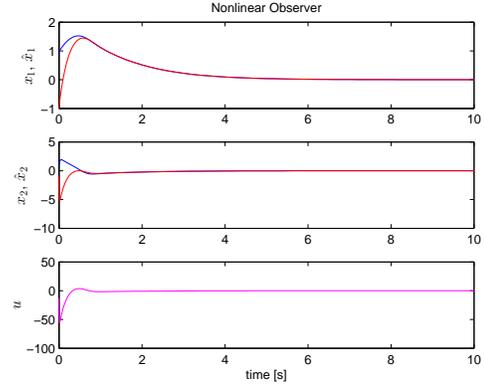
Fig. 8: blue: real states, red: estimated states
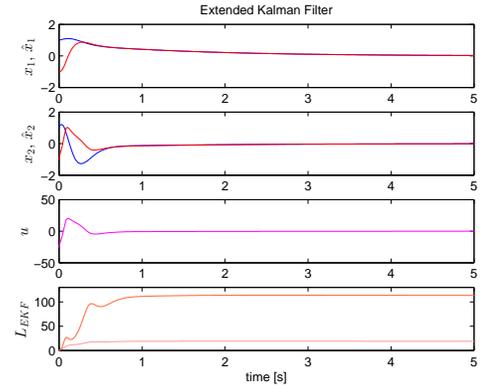
Fig. 9: blue: real states, red: estimated states

D. Surge

To visualize the surge phenomenon the controller gets turned off and the observers start with different initial conditions than the model: $x_{init} = \begin{bmatrix} 0.1 & 0 \end{bmatrix}$ and $\hat{x}_{init} = \begin{bmatrix} -0.1 & 0 \end{bmatrix}$. Both open-loop systems go into a limit cycle oscillation as can be seen in the Figures 10 and 11. It is easy to recognize that the nonlinear observer is superior compared to the EKF in estimating this oscillation. The performance differs a lot in this case, as can be viewed in the plot of the estimation errors for both observers in Figure 12.
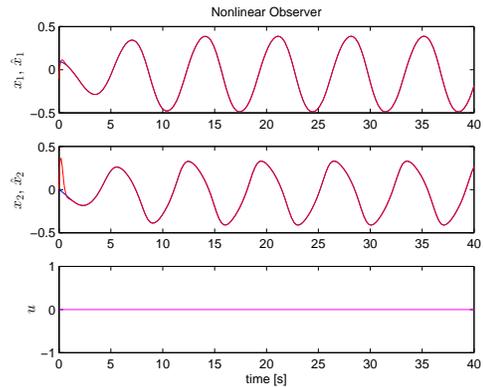
Fig. 10: blue: real states, red: estimated states
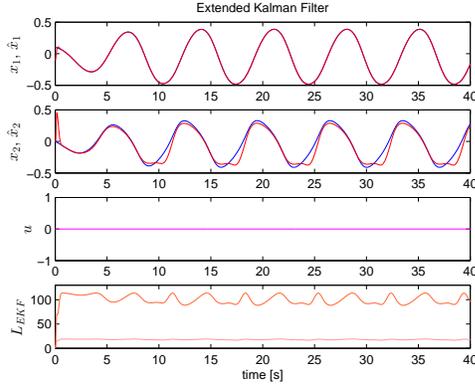
Fig. 11: blue: real states, red: estimated states
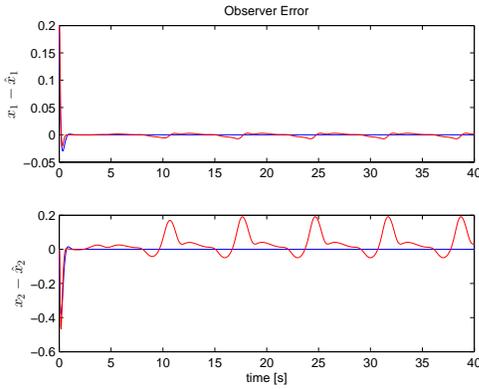
Fig. 12: blue: Nonlinear observer, red: EKF

VIII. CONCLUSION

In this paper we presented a locally asymptotically stable nonlinear observer for a Greitzer compressor model together with linear state feedback for surge control. The advantage of the nonlinear observer is that it is easy to implement. A further property gets clear when looking at the open loop simulation (surge case), where it showed better convergence properties than the Extended Kalman Filter: The estimation error of the EKF remained within a bound indicating stability (not asymptotic), whereas the estimation error of the nonlinear observer vanished giving asymptotic stability.

Simulations show that the nonlinear observer designed with the circle criterion gives at least the same performance like the in industry established and widely used EKF.

REFERENCES

[1] Murat Arcak and Petar Kokotovic. Nonlinear observers: a circle criterion design and robustness analysis. *Automatica*, 37:1923–1930, 2001.
[2] Bjørnar Bøhagen, Olav Stene, and Jan Tommy Gravdahl. A ges mass flow observer for compression systems: Design and experiments. In *Proceedings of the American Control Conference*, Boston, Massachusetts, USA, 2004.
[3] Bram de Jager. Rotating stall and surge control: A survey. In *Proceedings of the Conference on Decision & Control*, New Orleans, Louisiana, USA, 1995.
[4] Jan Tommy Gravdahl and Olav Egeland. Compressor surge control using a close-coupled valve and backstepping. In *Proceedings of the American Control Conference*, Albuquerque, New Mexico, USA, 1997.
[5] Edward M. Greitzer. Surge and rotating stall in axial flow compressors. part i: Theoretical compression system model. *Journal of Engineering for Power*, 98:190–198, 1976.
[6] Riccardo Marino and Patrizio Tomei. *Nonlinear Control Design: Geometric, Adaptive and Robust*. Prentice Hall Information and System Sciences Series. Prentice Hall Europe, Hertfordshire, 1995.
[7] Anton Shiriaev, Rolf Johansson, Anders Robertsson, and Leonid Freidovich. Output feedback stabilization of the moore-greitzer compressor model. In *Proceedings of the Conference on Decision & Control and the European Control Conference*, Seville, Spain, 2005.
[8] Anton Shiriaev, Rolf Johansson, Anders Robertsson, and Leonid Freidovich. Criteria for global stability of coupled systems with application to robust output feedback design for active surge control. In *Proceedings of the Conference on Control Applications*, Saint Petersburg, Russia, 2009.
[9] Jonathan Seth Simon. *Feedback stabilization of compression systems*. PhD thesis, Massachusetts Institute of Technology, Department of Mechanical Engineering, 1993.

APPENDIX

TABLE I: Simulation parameters

A_c	0.01 m^2
B	0.832 m^{-1}
H	0.18
K	-4.53
L	$\begin{bmatrix} -10.09 & -58.65 \end{bmatrix}^T$
L_c	3 m
Q_{EKF}	$\begin{bmatrix} 10^1 & 0 \\ 0 & 10^3 \end{bmatrix}$
R_{EKF}	0.1
U	80 s^{-1}
V_p	1.5 m^3
W	0.25
a_s	340 ms^{-1}
k_1	-1.037
k_2	0.864
k_3	5.76
x_{1_0}	0.533
x_{2_0}	0.3
β_1	0.3
β_2	8.9
γ	0.411
ε	-5
η	9
μ_1	1.83
μ_2	10.07
ν	80.11
ν_{bound}	40